

Correlated electron transport in coupled metal double dots

Alexei O. Orlov,^{a)} Islamshah Amlani, Geza Toth, Craig S. Lent, Gary H. Bernstein, and Gregory L. Snider

Department of Electrical Engineering, University of Notre Dame, 275 Fitzpatrick, Notre Dame, Indiana 46556

(Received 2 June 1998; accepted for publication 12 September 1998)

The electrostatic interaction between two capacitively coupled, series-connected metal double dots is studied at low temperatures. Experiment shows that when the Coulomb blockade is lifted, by applying appropriate gate biases, in both double dots simultaneously, the conductance through each double dot becomes significantly lower than when only one double dot is conducting a current. The conductance lowering seen in interacting double dots is compared to that caused by an external ac modulation applied to the double-dot gates. The results suggest that the conductance lowering in each double dot is caused by a single-electron tunneling in the other double dot. Here, each double dot responds to the instantaneous, rather than average, potentials on the other double dot. This leads to correlated electron motion within the system, where the position of single electron in one double dot controls the tunneling rate through the other double dot. © 1998 American Institute of Physics. [S0003-6951(98)04445-3]

In the last few years, much attention has been given to coupled Coulomb blockade systems; series and parallel connected metal and semiconductor systems were studied in various aspects.¹ Correlated transport in capacitively coupled Coulomb blockade systems was studied recently both theoretically² and experimentally,³ but the discussion was limited to the second-order (cotunneling) transport processes. Another example of a system utilizing correlated tunneling processes in coupled quantum dots is the basic cell of quantum-dot cellular automata (QCA).⁴ The basic cell of QCA consists of four dots situated at the corners of a rectangle, and charged with two excess electrons. Due to the Coulomb repulsion, the electrons stay in the two possible diagonal positions, which can be switched by applied input signal. A functional QCA cell was first demonstrated in Ref. 5. More recently, the cell consisting of the two identical capacitively coupled double dots (DDs), was studied.⁶ In addition to the possible applications, a QCA cell is an interesting model system allowing us to study interaction and correlation effects of single electrons. In this letter, we report an experimental study of correlated electron transport in a QCA cell described by Amlani *et al.*⁶

In contrast to previous work,^{2,3} which studied cotunneling in a similar system, in this letter, we study the interaction between DDs in the regime when single-electron tunneling occurs in both DDs simultaneously. This is accomplished by applying appropriate biases to the gates controlling the charge state of the system, so that both of the DDs are in the transitional state. We define a transitional state for a DD as a charge state where, if no source-drain bias is applied, an excess electron bounces between dots, spending half of its time on each of the dots. At finite temperature conductance through the DD in this state is nonzero due to a contribution to the conductance through excited states. We found that if both DDs are in the transitional state the conductance through each DD becomes significantly lower than when

only one DD is in its transitional state, with the other DD electrons “locked” by Coulomb blockade. To study the origin of this conductance reduction, we compare the conductance lowering observed for both DDs in the transitional state to that caused by an external *ac* modulation applied to the gates of one DD in the transitional state. The result supports the model that the conductance lowering for the DD in the transitional state is caused by the single-electron tunneling in the other DD. For noninteracting DDs, the conductance is limited by the tunneling rate of electrons through the DD, while in coupled DDs the tunneling rate is modified by the additional requirement that the excess electron on the other DD must be in the proper position before tunneling can take place. Thus, tunneling events in both DDs are strongly correlated and position of a single electron in one DD controls the tunneling rate in the other DD. The most interesting fact is that the conductance in one DD responds to the instantaneous potential changes on the other DD. The frequency of that process is determined by the single-electron tunneling rate, and is greater than 20 MHz even at millikelvin temperatures. On the contrary, the average potential cannot affect the tunneling in the other DD, since it is zero at the transitional state.⁷ This shows that coupled quantum dots can respond to rapidly changing input voltages, which suggests that the operating frequency of devices such as QCA can be very high.

Figure 1(a) shows the scanning electron microscopy (SEM) micrograph of the device; schematic diagram of the device and experimental setup is shown in Fig. 1(b). The device under study consists of two pairs of metal (Al) islands (dots)— D_1D_2 and D_3D_4 connected in series by tunnel junctions. The DDs are electrostatically coupled to each other by capacitors C_c . Al/AlOx/Al tunnel junctions are fabricated on an oxidized Si substrate using electron beam lithography and shadow evaporation.⁸ The area of the junctions is about $50 \times 50 \text{ nm}^2$. Measurements were performed in a dilution refrigerator with a base temperature of 10 mK.

Conductances of each DD were measured simulta-

^{a)}Electronic mail: orlov.1@nd.edu

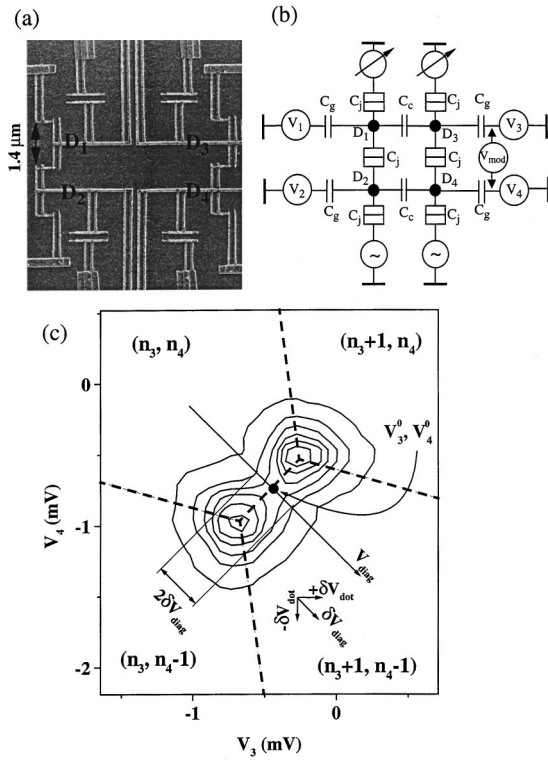


FIG. 1. (a) SEM micrograph of the device. (b) Schematic diagram of the device and experiment. (c) Contour plot of conductance through a double dot D_3D_4 as a function of gate voltages V_3 and V_4 ; (n_3, n_4) is the number of excess electrons on dots D_3 and D_4 .

neously using standard *ac* lock-in technique with $5 \mu\text{V}$ excitation, and a magnetic field of 1 T applied to suppress the superconductivity of Al. Capacitances of the circuit ($C_j \approx 1.44e/\text{mV}$, $C_c \approx 0.9e/\text{mV}$, $C_g \approx 0.45e/\text{mV}$) were determined from periods of Coulomb blockade oscillations and $I-V$ measurements.⁹ To suppress the effect of parasitic crosstalk capacitances between dots and nonadjacent gates, we used a charge cancellation technique described elsewhere.¹⁰

To understand the experiment, we need to look at the charging processes for one DD. By measuring the conductance through a DD as a function of the voltages applied to the DD gates V_3 and V_4 (we will consider DD D_3D_4 , but D_1D_2 is similar), we can determine the electron charge configuration within the DD. A contour plot of the conductance through D_3D_4 as a function of gate voltages V_3 and V_4 is shown in Fig. 1(c). At low temperatures ($kT \ll E_c$, where $E_c \sim 100 \mu\text{V}$ is the charging energy of D_3D_4) current flows through a DD only at the settings of the gate voltages where the Coulomb blockade is lifted. Due to capacitive coupling between dots each conductance peak splits in two.¹¹ Dashed lines in Fig. 1(c) delineate the regions where a particular configuration (n_3, n_4) is the ground state, with n_3 and n_4 representing the number of excess electrons on dots D_3 and D_4 , respectively.¹¹ An exchange of an electron between the two dots occurs along diagonal direction V_{diag} , while total charge on D_3D_4 remains constant along this direction.

As mentioned above, the conductance remains nonzero in the middle of the split peak at 50 mK (which we believe is the actual electron temperature in our experiment) due to a contribution to the conductance through excited states.

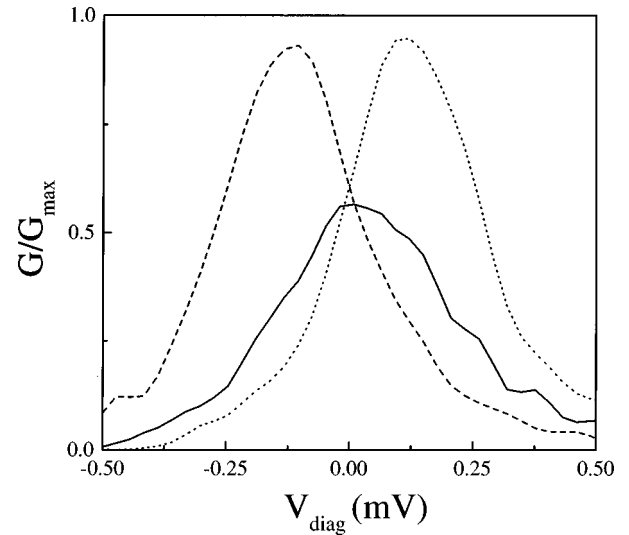


FIG. 2. Conductance through the D_3D_4 along V_{diag} for different charge states of D_1D_2 : dashed line— (n_1, n_2) ; dotted line— (n_1+1, n_2-1) ; solid line—transitional state.

Therefore, the region between each split peak forms a saddle point in $G-V_3-V_4$ space, which shows up as a conductance peak along V_{diag} on Fig. 1(c). We use this peak as a marker, which corresponds to a border between states with different electron configurations. We will concentrate on the transition region between the two charge configurations (n_3, n_4) and (n_3+1, n_4-1) . To set a DD in the transitional state, the working point [V_3^0, V_4^0 in Fig. 1(c)] must be at the saddle point of a split peak, on the border between two charge configurations (n_i, n_j) and (n_i+1, n_j-1) , where $i, j=1, 2$ and 3, 4.

Each time an electron hops from one island of a DD to the other, the electrostatic potential on the island losing the electron becomes more positive and the potential on the island gaining that electron becomes more negative with re-

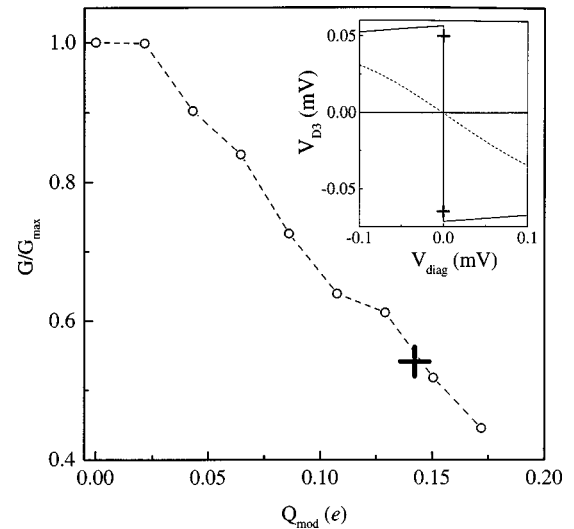


FIG. 3. Conductance peak height as a function of charge variation for DD D_3D_4 at $V_{\text{diag}}=0$, $T=10 \text{ mK}$, $f_{\text{mod}}=335 \text{ Hz}$. V_1, V_2 are set to lock electrons on D_1D_2 in the Coulomb blockade. Charge coordinate of the cross is the theoretically calculated charge variation produced by a single electron tunneling from dot D_1 to D_2 . **Insert:** Potential on D_3 vs V_{diag} : solid line—theory for 0 K, dashed line—theory for 50 mK, crosses show potential difference extracted from the external modulation experiment.

spect to ground. On average at the saddle point of a split peak, the theoretically calculated excess occupation of each dot is 50% with a voltage phase difference of 180° between them.⁷ In the transitional state, the potential on each dot as a function of time can be viewed as a series of voltage ‘‘pulses’’ with amplitude δV_D , corresponding to the presence or absence of an electron. The ‘‘duty cycle’’ of these pulses depends on V_{diag} . For $V_{\text{diag}}=0$, the duty cycle is 50%, since an electron has an equal probability to be at either dot of DD. The frequency of the pulses is defined by single-electron tunneling rate $\Gamma = kT/e^2 R_j$ (where $R_j \approx 1 \text{ M}\Omega$ is the resistance of a tunnel junction) and for $T=50 \text{ mK}$ is about 20 MHz.

Therefore, this situation can be viewed as if the potentials on one DD act as a time varying effective gate voltages for the other DD. On the charging diagram in Fig. 1(c), the effect of such switching potential on the adjacent DD corresponds to the two settings of effective diagonal gate bias $\delta V_{\text{diag}} = \pm[(+\delta V_{\text{dot}})^2 + (-\delta V_{\text{dot}})^2]^{1/2}$, where $+\delta V_{\text{dot}}$ is a change of the electrostatic potential on the dot losing and $-\delta V_{\text{dot}}$ on the dot gaining the electron (we define $V_{\text{diag}}=0$ for $V_3=V_3^0$, $V_4=V_4^0$). In response to the instantaneous change of the potentials $\pm \delta V_{\text{diag}}$ on $D_1 D_2$, the electron tunneling rate in $D_3 D_4$ reduces as evidenced by the reduction of conductance in Fig. 1(c). In effect, a negative potential on dot D_1 , due to the presence of an electron, prevents another electron from tunneling onto D_3 until the first electron moves to D_2 . As a result conductance of $D_3 D_4$ drops compared to the case when charge on $D_1 D_2$ is locked and potentials on D_1 and D_2 are fixed, as seen in Fig. 2. At the same time, if conductance through one DD were affected by only the average potential on the other DD, no conductance reduction is expected. Thus, according to the experiment of Fig. 2, transport of electrons through the system when both DDs are in the transitional state becomes strongly correlated, with the probability for an electron to tunnel through one DD dependent on the position of the excess electron on the other DD. The effect of conductance reduction is observed in all samples under study (a total of three samples). The correlation strength and conductance reduction depend on temperature and disappear at $kT \sim E_c$.⁷

At $V_{\text{diag}}=0$, we can model the conductance modulation caused by a single-electron switching in $D_1 D_2$ by applying a square-wave modulation with a 50% duty cycle to the gates V_3 and V_4 . The applied signals must be out of phase by 180° to imitate the electron hop from D_1 to D_2 . The potential difference produced by $D_1 D_2$ is $\delta V = V_{D_1} - V_{D_2}$, and the charge which affects the $D_3 D_4$ is therefore $\delta Q = \delta V C_c$. To mimic the same amount of charge variation, $\delta Q = \delta V_g C_g = \delta V C_c$, a signal of $\delta V_g = \delta V C_c / C_g$ must be applied to the gates. Gate voltages on $D_1 D_2$ are set to lock electrons there in Coulomb blockade to prevent any effects in $D_3 D_4$ caused by single-electron tunneling in $D_1 D_2$.

We apply a square-wave differential modulation signal between the gates V_3 and V_4 with a frequency of 100–10000 Hz, much lower than a single-electron tunneling rate. The result of this gate modulation experiment is shown on the Fig. 3 where the conductance of the $D_3 D_4$ measured at $V_{\text{diag}}=0$ is plotted versus the amplitude of applied charge modulation. The cross in Fig. 3 marks the conductance low-

ering observed in the experiment of Fig. 2. The observed conductance lowering was frequency independent up to 10 kHz (cutoff frequency of our experimental setup). The position of the cross confirms that the conductance lowering occurs due to the instantaneous potential variation caused by electrons tunneling through the other DD. The insert in Fig. 3 shows the theoretically calculated dot potential versus V_{diag} at 0 K. The theoretical results are obtained by minimizing the classical electrostatic energy for the array of islands and voltage leads. Finite temperature smears the transition region, but for $V_{\text{diag}}=0$, the instantaneous values of potential remain the same, jumping between ‘‘high’’ and ‘‘low’’ levels, while the average potential is zero. The crosses in the insert of Fig. 3 mark the amplitude of the normalized external modulation at which the conductance peak height matches that observed in Fig. 2 and shows good agreement with theory. Therefore, the external modulation experiment can be used to measure the potential difference between the dots, and provides further evidence that the conductance reduction is due to instantaneous potential variations.

In summary, we report the observation of correlated transport in the Coulomb coupled double dots. We found that when single-electron tunneling takes place in both DDs simultaneously the conductance through each of the interacting DDs drops. We explain this conductance lowering by electrostatic interactions between DDs, where the conductance through each of the DDs is affected by instantaneous changes of electrostatic potentials created by electrons tunneling through the dots in the other DD. We confirm this by an experiment where square-wave modulation was applied between the gates of DD to simulate potential changes caused by single-electron tunneling in the other DD, and find a good agreement with theoretical calculations. Our results suggest that coupled DD can respond to rapid changes of input voltages, implying very high operating frequencies of devices based on quantum dots, such as QCA.

This research was supported in part by DARPA, ONR (Grant No. N00014-95-1-1166) and NSF. The authors are grateful to W. Porod and J. Merz for stimulating discussions.

¹L. P. Kouwenhoven *et al.*, in *Proceedings of the Advanced Study Institute on Mesoscopic Electron Transport*, edited by L. L. Sohn, L. P. Kouwenhoven, and G. Schon (Kluwer, Dordrecht, 1997).

²D. V. Averin, A. N. Korotkov, and Yu. V. Nazarov, *Phys. Rev. Lett.* **66**, 2818 (1991).

³P. Delsing, D. B. Haviland, and P. Davidsson, *Czech. J. Phys.* **46**, 2359 (1996).

⁴C. S. Lent, P. D. Tougaw, W. Porod, and G. H. Bernstein, *Nanotechnology* **4**, 49 (1993).

⁵A. O. Orlov, I. Amlani, G. H. Bernstein, C. S. Lent, and G. L. Snider, *Science* **277**, 928 (1997).

⁶I. Amlani, A. O. Orlov, G. L. Snider, C. S. Lent, and G. H. Bernstein, *Appl. Phys. Lett.* **72**, 2179 (1998).

⁷G. Toth and C. S. Lent (unpublished).

⁸T. A. Fulton and G. H. Dolan, *Phys. Rev. Lett.* **58**, 109 (1987).

⁹C. Livermore, C. H. Crouch, R. M. Westervelt, K. L. Campman, and A. C. Gossard, *Science* **20**, 1332 (1996).

¹⁰G. L. Snider, A. O. Orlov, I. Amlani, G. H. Bernstein, C. S. Lent, J. L. Merz, and W. Porod, *Solid-State Electron.* **42**, 1355 (1998).

¹¹H. Pothier, P. Lafarge, P. F. Orfila, C. Urbina, D. Esteve, and M. H. Devoret, *Physica B* **169**, 573 (1991).